

Ion Diffusion Restricted by Time-Dependent Barriers in a Viscous Polyethylene-Based Liquid Electrolyte

Kikuko Hayamizu,^{*,†} Etsuo Akiba,[†] and William S. Price[‡]

AIST Tsukuba Center 5, National Institute of Advanced Industrial Science and Technology, Tsukuba 305-8565, Japan, and Nanotechnology Group, College of Science, Technology and Environment, University of Western Sydney, Penrith South 1797, Australia

Received August 26, 2003

Revised Manuscript Received October 14, 2003

Polymer–electrolytes for use in lithium rechargeable batteries have the potential ability to power portable devices, yet the molecular level details of the ionic conduction mechanisms, which lie at the crux of their functionality, are poorly understood (e.g., see refs 1–3 and references therein). Standard electrochemical theories fail to predict both the time dependence of the ionic conductivity and its correlation with the nature and time dependence of the diffusion coefficients of the individual species (i.e., anion, cation, and polymer) in such electrolytes. Consequently, the development of high-performance polymer–electrolyte batteries is hindered.

Four years previously, multinuclear NMR T_1 and pulsed gradient spin-echo (PGSE) NMR self-diffusion coefficient measurements of the liquid macromonomer (i.e., the “solvent”), lithium ion, and anion in the liquid electrolytes, (ethylene oxide)-*co*-(propylene oxide) (*m*(EO–PO), MW \sim 8000) doped with $\text{LiN}(\text{SO}_2\text{CF}_3)_2$ (LiTFSI) were performed in the temperature range 303–393 K and analyzed.² The flame-sealed samples were subsequently stored at room temperature. In the present article, we report the results of the NMR remeasurements. In the interim the spectrometer was upgraded affording significantly better signal-to-noise. The new NMR data reveal that the electrolyte has undergone significant structural relaxation in the intervening period and provides cogent information on the evolving molecular architectures that influence the conductivity and largely explains the nonideal behaviors. The present study is a significant extension of a recent study of the solid random-cross-linked version of the same electrolyte system.³ A detailed description of the experimental methods can be found elsewhere.^{2,3}

The resulting conceptual and “idealized” model of the electrolyte system is presented in Figure 1, ahead of the results, to allow more transparent discussion. The ^1H , ^7Li , and ^{19}F NMR T_1 values at 353 K were unchanged in the present measurements. The ^7Li and ^{19}F spin–spin relaxation profiles were unchanged and single exponential. However, while the decay of the ^1H NMR echo signals were also single exponential, they are apparently biexponential in the present measurements. At 323 K, the T_2 values (proportion) were 59 (0.09) and 14 ms (0.91) (previous data 19 ms) increasing to 91

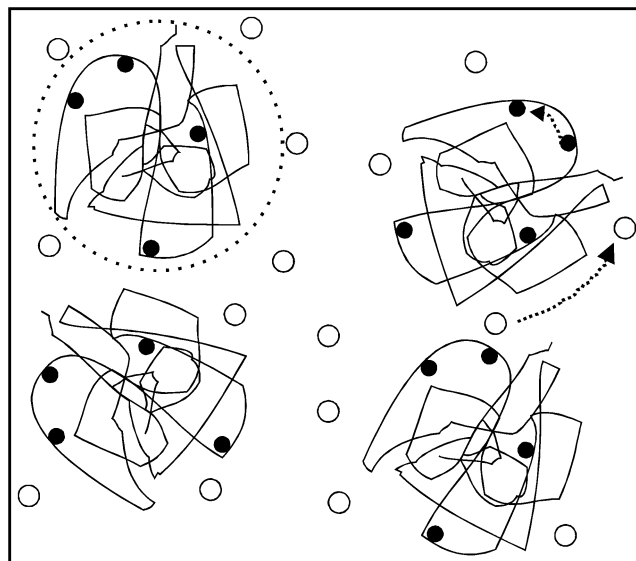


Figure 1. Conceptual model of the molecular environment in the polymer electrolyte at one particular instant of time. The salt (Li, solid circles; anion, open circles) induces the polymer (curved lines) to form hyperstructures. The lithium ions undergo curvilinear diffusion along the polymer chains in the hyperstructures whereas the anions undergo diffusion between voids created in the dynamic hyperstructure matrix. The hyperstructures continuously evolve, and a dashed circle has been placed around one of the hyperstructures to indicate a loose connection with a spherical restricting geometry.

(0.39) and 25 ms (0.61) (previous data 49 ms) at 353 K. Thus, the constancy of the T_1 values implies that the nanosecond-order motions in the local environment are essentially the same. The present biexponential nature of the polymer T_2 is consistent with increased structuring and perhaps heterogeneity. Both of these phenomena would result from the macromonomer becoming organized into hyperstructures.

PGSE NMR diffusion measurements, in contrast to relaxation measurements, are sensitive to motions occurring over the time scale of the diffusion measurement, Δ (millisecond order), and correspondingly larger distances. The short gradient pulse (SGP) approximation, in which motion during the magnetic gradient pulse of duration δ is neglected, provides a very intuitive framework for interpreting the experimental data. The echo attenuation, E , is given by the Fourier Transform of the diffusion propagator^{4,5} $P(\mathbf{r}_0, \mathbf{r}_1, t)$ with respect to the reciprocal space vector $\mathbf{q} = (2\pi)^{-1}\gamma\mathbf{g}\delta$ (m^{-1}),⁶

$$E = \int \int \rho(\mathbf{r}_0) P(\mathbf{r}_0, \mathbf{r}_1, \Delta) e^{i2\pi\mathbf{q}(\mathbf{r}_1 - \mathbf{r}_0)} d\mathbf{r}_0 d\mathbf{r}_1 \quad (1)$$

where $\rho(\mathbf{r}_0)$ is the equilibrium spin-density, and the integral is taken over all starting (\mathbf{r}_0) and finishing (\mathbf{r}_1) positions, γ is the gyromagnetic ratio, and \mathbf{g} is the magnitude of the pulse. For free (i.e., “Fickian”) diffusion the mean square displacement (msd) scales linearly with Δ , and the PGSE attenuation profile (from eq 1) is a single exponential, viz.

$$E = \exp(-(\Delta) D q^2) \quad (2)$$

In contrast, for diffusion within confining geometries, the msd does not scale linearly with time. And the

* Corresponding author. E-mail: hayamizu.k@aist.go.jp. Telephone: +81-29-861-6295. Fax: +81-29-861-6295.

[†] National Institute of Advanced Industrial Science and Technology.

[‡] University of Western Sydney.

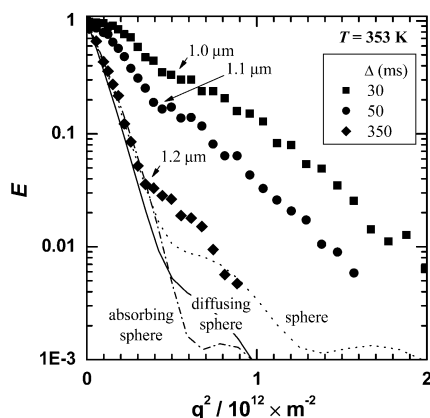


Figure 2. ^1H PGSE attenuation profiles for the polymer in LiTFSI-*m*(EO-PO) Li/O = 0.05 at 353 K. The diffractive behavior of the attenuation plots becomes more pronounced at longer Δ and lower temperatures (not shown). Only the simulations for the $\Delta = 350$ ms data are shown. The dotted line is a simulation using the sphere model with $D = 1.7 \times 10^{-12} \text{ m}^2 \text{ s}^{-1}$ and $a = 1.1 \mu\text{m}$. The solid line was simulated using the diffusing sphere model with $D = 1.7 \times 10^{-12} \text{ m}^2 \text{ s}^{-1}$ and $a = 1.1 \mu\text{m}$ and a sphere diffusion coefficient of $D_m = 1.0 \times 10^{-13} \text{ m}^2 \text{ s}^{-1}$. The dot-dash line is a simulation using the absorbing wall model with a radius of $a = 1.15 \mu\text{m}$, and M (ms^{-1}) is the wall relaxation parameter such that $Ma/D = 7$. Smaller D values, although providing a better fit to the shorter Δ data at low q values, preclude the simulation of diffraction effects.

attenuation profile is more complex and may exhibit diffractive behavior at well-defined values of q with respect to the shape and characteristic dimension of the restricting geometry, for example, the radius a in the case of a sphere.

Four years ago, the PGSE profiles of the polymer obtained using a modified Hahn echo pulse sequence were single-exponential permitting the determination of self-diffusion coefficients (e.g., $8.5 \times 10^{-13} \text{ m}^2 \text{ s}^{-1}$ at 353 K and $\Delta = 50$ ms) for the signal with a single T_2 , and the coefficients could not be determined below 323 K due to increasing nonexponential behavior. At present, using a stimulated-echo pulse sequence, the PGSE profiles contain contributions from both the short and long T_2 components. As shown in Figure 2, the profiles were nonexponential at all Δ values and temperatures, and exhibited diffraction like phenomena that became more pronounced as the temperature decreased. The observation of diffractive minima is extremely informative about the microscopic structure of the polymer electrolyte. First, on the time scale of Δ , the species exhibiting the minima is restricted to a confined space. Second, the characteristic distance(s) do not change much on the time scale of Δ , which indicates there would not be too much polydispersity in size,⁷ else the minima would be smeared out. Three restricted diffusion models of varying complexity were used to simulate the electrolyte model proposed in Figure 2: (1) diffusion within a sphere,^{8,9} (2) diffusion within a sphere with absorbing walls,¹⁰ and (3) diffusion within a sphere which is itself diffusion.¹⁴ The sphere model and variants were chosen because, although clearly too simplistic for modeling the present system, out of the common simple geometries the sphere model gives the first diffractive minimum at the lowest values of q ($\approx 0.71/a$). Analysis of the diffractive minima using the sphere model at 323 K give the radius as (30 ms, $0.9 \mu\text{m}$; 50 ms, $0.9 \mu\text{m}$; 350 ms, $1.0 \mu\text{m}$) and at 353 K give (30 ms, $1.0 \mu\text{m}$; 50 ms, $1.1 \mu\text{m}$; 350 ms, $1.2 \mu\text{m}$). Simulations were attempted for

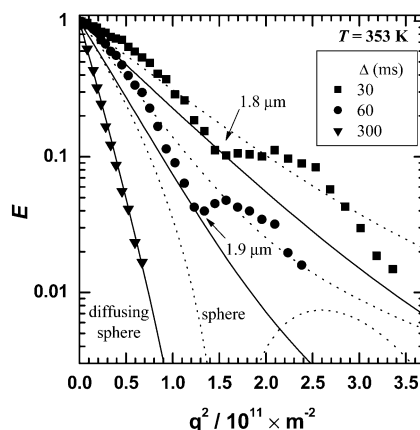


Figure 3. ^7Li PGSE profiles of LiTFSI-*m*(EO-PO) Li/O = 0.05 at 353 K at three Δ values. Simulations were performed using the sphere model (dotted lines) with $D = 1.5 \times 10^{-11} \text{ m}^2 \text{ s}^{-1}$ and the diffusing sphere model (solid lines) with $D = 1.5 \times 10^{-11} \text{ m}^2 \text{ s}^{-1}$ and a sphere diffusion coefficient of $D_m = 2.7 \times 10^{-12} \text{ m}^2 \text{ s}^{-1}$. The $\Delta = 30$ and 300 ms data were simulated with $a = 1.8 \mu\text{m}$ and the $\Delta = 60$ ms data were simulated with $a = 1.9 \mu\text{m}$.

the three models and the results obtained for the 350 ms data sets are shown in the figure. It is reasonable to expect that the hyperstructure matrix is slowly changing, and of the three models, the diffusing sphere model should be the closest, albeit very simplistically, to emulating transient spherical restriction.

Previously, the lithium PGSE profiles were single exponential in the temperature region 333–363 K. At present, the profiles were nonexponential and exhibited Δ dependence at 353 K as shown in Figure 3. Diffractive minima are clearly evident at shorter Δ . Analysis of the diffractive minima give radii of the order of 1.7 – $1.9 \mu\text{m}$. Evidence of the minima disappears by $\Delta = 75$ ms and the profiles appear to become more exponential. However, the lack of minima at longer Δ likely results from the experimental q values being too small to achieve diffractive effects. Nevertheless, at $\Delta = 300$ ms the PGSE profile was exponential giving an apparent self-diffusion coefficient of $5.2 \times 10^{-12} \text{ m}^2 \text{ s}^{-1}$ which is slightly larger than the previous value of $4.5 \times 10^{-12} \text{ m}^2 \text{ s}^{-1}$ measured at $\Delta = 50$ ms.

The ^7Li PGSE attenuation profiles for the lithium diffusion were measured at $\Delta = 50$ ms in the temperature range 313–353 K, and selected data are plotted in Figure 4. Diffractive behavior is observed at all temperatures but the apparent radii increase from $1.7 \mu\text{m}$ (313 K) to $1.9 \mu\text{m}$ (343 K), and the diffractive minima become more sharply defined. This trend is consistent with the radii formed by the polymer chains increasing with temperature.

Previously, the anion diffusion profiles were consistent with a single freely diffusing component at every temperature but Δ -dependent with the values decreasing with increasing Δ and ultimately approaching a long-time equilibrium value. This is similar to that observed in the cross-linked system,³ and implies that the anions are undergoing some form of anomalous diffusion^{11,12} due to the dynamic hyperstructure matrix within which they are diffusing. However, in the new measurements the anion diffusion coefficient was independent of Δ (between 1.64×10^{-11} and $1.74 \times 10^{-11} \text{ m}^2 \text{ s}^{-1}$ for $\Delta = 25$ – 100 ms at 343 K, but previously they changed from 1.7×10^{-11} ($\Delta = 100$ ms) to $2.2 \times 10^{-11} \text{ m}^2 \text{ s}^{-1}$ ($\Delta = 25$ ms)). The purely Fickian behavior of the

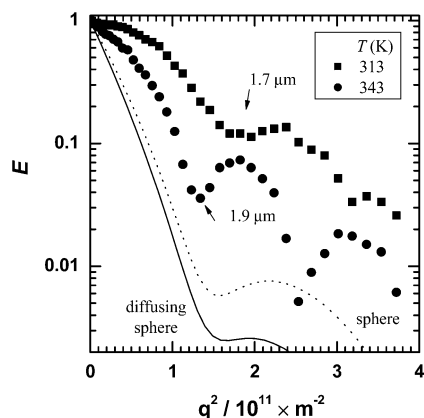


Figure 4. ^7Li PGSE profiles of LiTFSI-*m*(EO-PO) Li/O = 0.05 at 313 and 343 K measured with $\Delta = 50$ ms. Simulations were performed with the sphere model (dotted line) with $D = 5.0 \times 10^{-11} \text{ m}^2 \text{ s}^{-1}$ and $a = 1.9 \mu\text{m}$ and the diffusing sphere model (solid line) with $D = 5.0 \times 10^{-11} \text{ m}^2 \text{ s}^{-1}$ and a sphere diffusion coefficient of $D_m = 2.7 \times 10^{-12} \text{ m}^2 \text{ s}^{-1}$ and $a = 1.9 \mu\text{m}$.

anion in contrast to that of the polymer and cation indicates that it diffuses outside of the hyperstructures.

The data are consistent with the lithium salt inducing the polymer to form dynamic hyperstructures. The anions diffuse freely through the voids in the dynamic matrix and undergo Fickian diffusion, whereas the lithium ions undergo (time-dependent) curvilinear diffusion¹³ along the polymer chains. This conceptual model affords some hints to the intelligent design of electrolyte systems. In particular, given that the anions

dominate the conductivity, the polymers need to be designed so that the voids are such that the anion diffusion is enhanced while leaving the cation localized to the polymer hyperstructures so that conduction is not reduced by ion pairing. Fast lithium conduction, however, is important to produce rechargeable lithium batteries.

References and Notes

- (1) Videa, M.; Xu, W.; Geil, B.; Marzke, R.; Angell, C. A. *J. Electrochem. Soc.* **2001**, *148*, A1352–A1356.
- (2) Hayamizu, K.; Sugimoto, K.; Akiba, E.; Aihara, Y.; Bando, T.; Price, W. S. *J. Phys. Chem. B* **2002**, *106*, 547–554.
- (3) Hayamizu, K.; Akiba, E.; Bando, T.; Aihara, Y.; Price, W. S. *Macromolecules* **2003**, *36*, 2785–2792.
- (4) Kärger, J.; Heink, W. *J. Magn. Reson.* **1983**, *51*, 1–7.
- (5) Price, W. S. *Concepts Magn. Reson.* **1997**, *9*, 299–336.
- (6) Tanner, J. E.; Stejskal, E. O. *J. Chem. Phys.* **1968**, *49*, 1768–1777.
- (7) Price, W. S.; Stilbs, P.; Söderman, O. *J. Magn. Reson.* **2003**, *160*, 139–143.
- (8) Balinov, B.; Jönsson, B.; Linse, P.; Söderman, O. *J. Magn. Reson.* **1993**, *A 104*, 17–25.
- (9) Balinov, B.; Jönsson, B.; Linse, P.; Söderman, O. *J. Magn. Reson.* **1994**, *A 108*, 130.
- (10) Callaghan, P. T. *J. Magn. Reson.* **1995**, *A 113*, 53–59.
- (11) Kärger, J.; Fleischer, G.; Roland, U. PFG NMR Studies of Anomalous Diffusion. In *Diffusion in Condensed Matter*; Kärger, J., Heitjans, P., Haberlandt, R., Eds.; Vieweg: Braunschweig, Germany, 1998; pp 144–168.
- (12) Havlin, S.; Ben-Avraham, D. *Adv. Phys.* **2002**, *51*, 187–292.
- (13) Callaghan, P. T. *Principles of Nuclear Magnetic Resonance Microscopy*; Clarendon Press: Oxford, England, 1991.
- (14) Manuscript in preparation.

MA035265N